Submitted to Investigative Ophthalmology & Visual Science

Morphometric Analysis of Lipoprotein-like Particle Accumulation in Aging Human Macular Bruch's Membrane

Jiahn-Dar Huang [a]
Christine A. Curcio [b]
Mark Johnson [a]

[a] Department of Biomedical Engineering
Northwestern University
Evanston IL USA

[b] Department of Ophthalmology
University of Alabama School of Medicine
Birmingham AL USA

Short Title: Analysis of Lipoprotein-like Particle Accumulation in Bruch's Membrane

Keywords: age-related maculopathy, age-related macular degeneration, lipid, morphometry

Partial results were presented at ARVO 2006 and 2007.

Corresponding Address:
Mark Johnson, Ph.D.
Department of Biomedical Engineering
Northwestern University
2145 Sheridan Road
Evanston IL 60208-3107
(847) 467-7143; FAX (847) 491-4928
E-mail: m-johnson2@northwestern.edu

Abstract

PURPOSE. To determine the size and regional distribution of lipoprotein-like particles (LLPs) that accumulate with age in Bruch's membrane (BrM).

METHODS. The quick-freeze/deep-etch method was used to prepare specimens of human BrM (ages 27-78) for electron microscopic examination. We used stereologic methods to analyze the resulting micrographs and determine the age-related changes of the LLP volume fraction and diameter distribution in various locations in BrM.

RESULTS. The volume fraction occupied by LLPs was found to increase monotonically with age in both the inner collageneous layer (ICL) and elastic layer (EL) but not in the outer collageneous layer (OCL). The mass of total LLP-associated lipids in BrM also increased with age. There was a modest increase in LLP size with age.

CONCLUSIONS. The pattern of accumulation of particles was consistent with a retinal pigment epithelium (RPE) source for the LLPs. This would explain why once the EL and ICL were filled with particles, LLPs continued to accumulate near the RPE but no further accumulation was found in the OCL. The quantity of LLP-associated lipids found in BrM accounts for a large portion of the accumulated lipids measured in this tissue. The age related increase in LLP size was likely due to the higher particle volume fraction in older eyes promoting the probability of particle fusion.

INTRODUCTION

Bruch's membrane (BrM) is a thin layer of connective tissue located between the retinal pigment epithelium (RPE) and choroid. This tissue collects abundant quantities of lipid-rich deposits with advancing age.[1-5] Higher quantities of lipid deposits are found in the macular region,[2, 3, 6] and these deposits are postulated to compromise the metabolic transport through this region that is important for the health of RPE and photoreceptor cells.[4, 7-12]

In our previous studies, we used the quick-freeze/deep-etch (QFDE) technique, a method that preserves the ultrastructure of BrM to characterize the age-related changes of the tissue.[4-6] We found that two major types of deposits, lipoprotein-like particles (LLPs) and small granules, accumulate with age in BrM.[5] LLPs were of particular interest because they are a lipid-rich material.[5, 13]

Our previous work[4-5] suggested that the age-related accumulation of LLPs in BrM first fills the interfibrillar spacing of the elastic layer (EL) and then progressively fills the inner collagenous layer (ICL), ultimately leading to the formation of a "lipid wall" between the ICL and the basal lamina of the RPE (BL-RPE). While LLPs were found in the outer collagenous layer (OCL) in younger eyes, no further age-related accumulation was seen in this region. These observations suggested that the source of the LLPs was in the RPE.

The goal in the current study was to examine this result quantitatively. We used stereological methods to determine the volume fraction of LLPs seen in the images of ICL, EL and OCL prepared by QFDE. As our previous studies indicated that the LLP sizes were not uniform and that the LLPs were capable of fusing to form larger particles,[5] we also determined the particle diameter distribution in each of the three central layers of BrM. These studies allowed us to demonstrate the age-related variations of the LLPs in human macular BrM.

MATERIALS AND METHODS

Human Eye Tissue

Human eye tissues used in this study were obtained from Alabama Eye Bank and preserved within 4 hours post-mortem. Eyes containing drusen larger than 63 μm or any other grossly visible chorioretinal pathology of significance were excluded. In addition, we excluded eyes from donors with diabetes or receiving artificial respiration longer than 5 days. A total of 12 normal eyes, aged from 27 to 78 yr with two eyes from each decade of human life as previously described,[5] were analyzed (Table 1).

Tissue Processing

After the removal of the anterior segment of each eye, the posterior segment was preserved by immersion in 0.1 M phosphate buffer solution with 2.5% glutaraldehyde and 1% paraformaldehyde for at least 24 hours. We then dissected the macular region, including the retina, RPE, BrM, the choroid, and the sclera into sixteen 2×2 mm square blocks for QFDE and thin-sectioning processing.

For tissue blocks processed by QFDE, the retina was carefully removed from the tissue using fine forceps. The remaining RPE-BrM-choroid-sclera complex was slammed frozen in liquid nitrogen (-196°C) using a Leica EM MM80E (Leica Microsystems Inc., Bannockburn, IL). We then transfer the frozen tissue, with the RPE side facing up, into a freeze-fracture/deep-etch device (Cressington CFE-60, Cressington Scientific Instruments Ltd., Watford UK) held at a vacuum level of 10^{-7} mbar. The tissue block was fractured at low oblique angles using a cold razor blade and then etched at–95°C for 25 minutes to reveal BrM. Rotary shadowing using platinum/carbon mixture at 20° to the tissue surface and backed by carbon from above was used to make a replica of exposed BrM ultrastructure. The replica along with the tissue was immersed into the digestion solution (water/bleach = 1:1) for at least two hours to remove the biological

tissue. The remaining replica pieces were picked up by copper hexagonal grids, washed in water, air dried, and examined using a JEOL-100 CX (JEOL USA, Peabody MA) transmission electron microscope. Stereo micrograph pairs (±6°) of original magnification of ×8000 of the QFDE replica were scanned (AGFA Duoscan T2500) in TIFF mode. In order to improve image contrast, we use Photoshop CS (Adobe Systems Incorporated, San Jose CA) to equalize the digitized images.

Thin-sectioning TEM preparation was also applied to one or two tissue blocks of each eye. In this preparation, the fixed tissue blocks were postfixed either in 1% osmium and 0.125% potassium ferricyanide or by osmium-tannic acid-paraphenylenediamine (OTAP).[14] One micrometer-thick sections of the tissue were stained with 1% toluidine-blue-O in 2% sodium borohydrate. We examined the thin sections using a JEOL1200 EXII (JEOL USA, Peabody MA) or a Hitachi 7000 (Hitachi High Technology America, Pleasanton CA) electron microscope. Representative negatives of BrM cross-sections (Kodak EM film 4489, Eastman Kodak Company, Rochester NY) were scanned with a PowerLook 1100 scanner and Umax Magiscan 4.5 (Umax Technology, Dallas TX).

Image Processing and Stereological Analysis

Since very few LLPs were observed in the BL-RPE and the basal lamina of the choriocapillaris (BL-CC),[5] only images from the ICL, EL, and OCL were selected for LLP quantification. For each layer of each eye, at least three QFDE images were used to evaluate the LLP volume fraction seen in that layer. The OCL images of a 50 yr eye were not available due to technical difficulties. Images of the lipid wall were not included in these evaluations, as the depth of field necessary for the stereology could not be determined from these densely packed images.

The depth of field of QFDE images was greater than the characteristic size of the objects being measured in the images. As such, since the images are two-dimensional projections of a three-dimensional set of objects, stereological correction is required to determine the volume fraction of LLPs in an image. Overby and Johnson[15] developed methods for determining the volume fraction of a set of three-dimensional objects (ϕ) from the volume fraction measured on two-dimensional projections of these objects (ϕ'). We used their methodology, but considered only the volume fraction of the LLPs in images of Bruch's membrane.

To determine ϕ of the LLPs in a region, we required measurements of the fraction of the image covered by LLPs (ϕ'), the total perimeter of these particles per unit image area (α'), and the depth of field of the image (D_f). In order to evaluate ϕ' and α' for a particular image, the LLPs were visually identified and then traced using a mouse. An example is shown on Figure 1. ImageJ (NIH) was then used to determine the area and perimeter of each LLP. For each micrograph, the area and perimeter of all LLPs in that micrograph were summed and then divided by the total image area to obtain the values of ϕ' and α' of the image. The values of ϕ' and α' of each layer of each eye were determined by the weighted average of ϕ' and α' values of each image, with the image area as the weighted factor.

The detailed method to measure D_f of a QFDE images is described in Overby et al.[16] In the current study, for each EM image evaluated for ϕ' and α', three 500 × 500 nm regions were randomly selected in the image. Stereo images (±6°) of the region were overlapped in Photoshop CS. Two relatively nearby features on a micrograph were identified (within 100 nm of one another) and the distance between these two features was measured on both stereo images using ImageJ. The difference between these two length (Δl) could then be related to the vertical distance between these two structures using the relationship $\Delta y = \Delta l / 2\sin\theta$ ($\theta = 6°$). Three such measurements were made on each of the 3 regions of each micrograph. The depth of the field D_f

of each layer of each eye was then determined as the highest value of Δy obtained in all 27 measurements in the three images of each layer.

The following equations[15] were used to relate the measured parameters to the volume fraction of the LLPs in each layer of each eye:

$$\phi' = 1 - (1 - \phi)\exp\left(\frac{-\alpha D_f}{4(1-\phi)}\right) \quad (1)$$

$$\alpha' = \frac{\alpha\pi}{4}\exp\left(\frac{-\alpha D_f}{4(1-\phi)}\right)\left(1 + \frac{2\alpha D_f}{3\pi\phi} + \frac{\alpha D_f}{4(1-\phi)}\right) \quad (2)$$

The form of equations (1) and (2) are appropriate for spherically shaped particles,[15] a reasonable approximation for LLPs. Once the values of ϕ', α', and D_f were determined, only two unknowns, ϕ and α, remained. The two unknown values were then calculated by solving equation (1) and (2) using Matlab (MathWorks, Natick MA).

Determine LLP Diameter and Size Distribution

Only individual, non-overlapped particles seen in the images were considered for the determination of the LLP diameters. The projected area of a particle (*a)* was measured using ImageJ. Because most of LLPs seen in BrM prepared by QFDE were not sectioned by fracturing (as determined from the particle diameter distributions such as seen in Figure 6), stereological correction was not used for the measured particle areas. The particle diameter *D* was determined from the relation: $a = \pi D^2/4$, as LLPs were considered as spheroids in the current study. The average value of *D* for LLPs was determined in each of the three layers (ICL, EL and OCL) of each eye.

To determine the distribution of particle sizes, the LLPs in a layer of a particular eye were divided into groups with each group containing particles of similar diameters in 10 nm intervals from 0 to 300 nm. To generate the diameter distribution, the number of particles in each interval was divided by the total number of LLPs in that layer of that eye. For each layer, the age-related changes in LLP diameter distribution were presented in three groups: 20-40 yr, 40-60 yr, and 60-80 yr. The histogram of each age group was obtained from the average of the four eyes in that group, except the OCL of 40-60 yr that contained only three sample eyes.

Estimate of the Total Quantity of LLP-associated Lipids in BrM

Holz et al. reported values for the total lipid content of macular BrM and choroid.[2] We used the morphometrically-determined values of LLP size and volume in each layer to estimate the total quantity of LLP-associated lipid in BrM (Q) for comparison to their measurements.

The total quantity of lipid in LLPs found in BrM was estimated as:

$$Q = \sum_i \phi_i \times l_i \times A \times \sigma \times 0.85 \qquad (3)$$

where i represents the individual layers of BrM (ICL, EL, OCL), ϕ_i is the volume fraction of lipid in the ith layer, l_i is the thickness of the ith layer, A is the tissue area, and σ is the density of the LLP particles. We assumed that the density of the LLPs and the lipid-protein ratio of each LLP were similar to the average of LDL and VLDL.[17-20] Therefore the value of σ was set equal to 1 g/ml, and the constant 0.85 was used as an estimate of the lipid fraction of a LLP.[20] In order to compare our results to Holz et al.[2], we assumed the tissue area A as a 7 mm diameter circle since a trephine of the same diameter was used to obtain tissues in that study.

The layer thickness of the ICL, EL and OCL were measured from three cross-section thin-sectioning TEM images of each eye. The evaluator was unaware of the donor age when measuring the layer thickness. The measurements were taken using a vernier caliper (BEL-ART Scienceware) to evaluate the thickness of each layer seen on three 7500× micrographs of BrM cross-sections expanded onto A3+ size (13" ×19") papers. We then measured the layer thickness of five randomly selected locations on each micrograph print. Measurement of the OCL thickness avoided the intercapillary pillars. The thickness of each layer of each eye was determined as the average value of the fifteen measurements on TEM images.

Statistical Analysis.

Statistical comparisons between groups were done using a two-tailed Student t-test. Linear regression was used to investigate correlations between variables and to determine correlation coefficients (r) and significance of such correlations (p). We considered results as significant for $p < 0.05$.

RESULTS

Age-related changes of LLP volume fraction in individual layers

The results of the stereological analysis of the images of human BrM prepared by QFDE were listed in Table 2. Figure 2 showed the age-related changes of ϕ in the different layers of BrM. The LLP volume fraction of both the ICL ($p = 0.001$) and EL ($p = 0.01$) increased monotonically with donor age (Fig. 2A and B). However, unlike the ICL and EL, the ϕ value of the OCL appeared to increase before age 60 and then decrease thereafter (Fig. 2C). Figure 2D showed the data for the OCL when separating the samples into three groups with each group covered two decades of donor ages. Use of the Student's t-test indicated significant differences between the averaged ϕ values in both the 20-40 yr vs. 40-60 yr ($p = 0.006$) and the 40-60 yr vs. 60-80 yr ($p = 0.046$) groups, showing the highest value of ϕ in the 40-60 yr group.

Comparison between layers

In our previous study, we reported that the distribution of LLP depositions appeared different from layer to layer as did the evolution of these deposits with increasing donor age.[5] In order to further examine this issue, we compared the ϕ values of the different layers in three groups of eyes, under 40, 40-60, and over 60 yr. In eyes 20-40 yr, the ϕ values in the EL (2.1% ± 1.0%, mean ± SD, n = 4) and OCL (1.4% ± 0.8%, n = 4) were higher than in the ICL (0.8% ± 0.3%, n = 4) (Fig. 3A), with a significant difference seen between the EL and ICL ($p = 0.042$). In the 40-60 yr group, the ϕ values in three layers were all similar, with the EL again having the highest concentration of LLPs (ICL: 7.2% ± 4.5%, n = 4; EL: 9.3% ± 2.7%, n = 4; OCL: 7.0% ± 2.3%, n = 3) (Fig. 3B). In the 60-80 yr group, the ϕ values of both the ICL and EL were higher than in the younger eyes (12.7% ± 3.8% (n = 4) and 13.7% ± 5.6% (n = 4), respectively), and

they were significantly higher than the ϕ value of the OCL (3.2% ± 1.6% (n = 4); p = 0.003 for ICL vs. OCL; p = 0.011 for EL vs. OCL) (Fig. 3C).

Total LLP-Associated Lipids in BrM

With values of the volume fraction ϕ in each of the layers determined, we could evaluate the quantity of LLP-associated lipids in macular BrM of each eye by using equation (3). As the basal lamina of the RPE and choriocapillaris contained very few LLPs[5], the small contribution of these layers to the total quantity of LLP-associated lipids was neglected. Figure 4 shows that the estimated quantity of LLP-associated lipids in BrM (Q) increased with donor age, as expected (p = 0.001). Note that these values do not include the LLPs in the lipid walls found in the oldest eyes. We find both the trend and the level of the Q values (0.6 – 13.0 μg) are in good agreement with the results for the lipids in BrM/choroid measured by Holz et al.[2]

Size distribution of LLPs and age-related changes

The age-related changes of average particle diameter D in individual layers are shown in Figure 5. Particle diameter varied in size from approximately 40 to 100 nm without a significant tendency to increase with donor age. Examining the size distribution of LLP (Fig. 6) indicated that the distribution of particle size in all three layers broadened between ages 20-40 yr and 40-60 yr. However, the distribution in the EL and OCL did not appear to change much between ages 40-60 yr and 60-80 yr. We have previously reported that LLPs appear to fuse to form larger particles.[5] Since LLP fusion might be promoted by higher LLP volume fraction, we examined the correlation between LLP volume fraction and average particle diameter in the different layers. As shown in Figure 7, a significant relationship (p = 0.013) was found, but the correlation coefficient between these two parameters is not very strong (r = 0.41).

DISCUSSION

In this study, we showed that a major age-related accumulation of lipoprotein-like particles occurred in the ICL and EL of BrM with a lesser accumulation in the OCL (Fig. 2). We did not find a significant increase of the average LLP size with aging. In addition, we were able to estimate the total amount of LLP-associated lipid accumulated in Bruch's membrane. The estimated lipid amount increased with donor age and was similar to the measurements of the total lipid content of BrM-choroid using a direct assay approach (Fig. 4).[2]

A prominent result of this study was the steady increase of LLP volume fraction with donor age in the ICL and EL (Fig. 2). However, in the OCL, the volume of particles in this region appeared to increase in younger eyes but then decrease in older tissues. The increase of LLP amounts in ICL and EL with age eventually made these two regions the major locations of LLP deposition in BrM (Fig. 3).

The mechanism causing the inhomogeneous distribution of LLP accumulation in the layers of BrM remains to be determined. One explanation may relate to the origin and direction of transport of these particles. In our previous ultrastructural characterization of the LLP accumulation process in BrM, we postulated that the LLPs were likely originated as waste products secreted from the RPE for transport to the choriocapillaris. As such, when the interfibrillar spaces of the EL and ICL become filled with LLPs and other debris[5], further transport through BrM would be limited by this obstruction, and thus LLPs would begin to accumulate in the ICL region, ultimately leading to formation of the lipid wall.

Not only would this mechanism explain the relatively rapid increase in the LLP content of the ICL after age 40, but might also explain why the age-related change in the volume fraction of LLP in the OCL shows a very different trend (Figure 2C). Since particles in the OCL still have access to the choriocapillaris and intercapillary pillars, they can be cleared over time from this region, while further LLP transport into this region is inhibited by obstruction at the EL.

Support for an RPE origin of LLP particles is found in recent studies of the cholesterol composition of LLPs found in BrM. Li et al. demonstrated that upon density gradient ultracentrifuge these particles contain a cholesterol profile distinct from that of plasma lipoproteins (including low-density lipoproteins, LDLs) and postulated that these particles originated in the RPE.[15]

Further support for this theory may come from our findings of the distribution of LLP diameters (Fig. 6). The vast majority of the particles are much larger than size of LDL particles (23 nm),[20] even in the youngest eyes examined. This is true in all three layers examined. This result suggests that, unlike other connective tissues in the body[21], the inclusions seen in BrM are unlikely to be plasma-originated LDLs.

We estimated the total quantity of lipids in the LLP that accumulated with age in BrM by using the volume fraction data and the thickness of each layer measured in donor eyes. Since we selected the highest value of the depth of the field measured in QFDE images and did not include the lipid wall in our calculations, our estimate of lipid amount in macular BrM is conservative. Nevertheless, we find the quantity of LLP-associated lipids in the tissue increases with age (Fig. 4) and is in a similar range as the total lipid amount obtained from lipid extraction method and thin-layer chromatography assay.[2] We caution that this comparison involved assay results which remain to be confirmed, both with regard to the absolute levels[3] and the composition[13, 22] of the lipids recovered. Despite these shortcomings, the overall similarity between the morphological and biochemical results suggests that the LLPs may account for a large portion of the lipids that accumulate with age in BrM.

The mechanism of the accumulation of LLPs in BrM remains unknown. Nevertheless, our results suggest that the RPE-originated lipid-rich materials are collected with aging and represent a large portion of lipids found in the tissue. The accumulation of these particles likely leads to the formation of a hydrophobic barrier[10] within BrM, compromising the metabolic transport

through the area. This particle accumulation is also likely responsible for the age-related increase in hydraulic resistivity that has been reported.[23] Further studies are warranted in order to investigate the mechanism of deposition and the influence this deposition has on transport processes in this region.

Acknowledgement

The authors would like to thank Zaid Siddik, Melissa F. Chimento, and J. Brett Presley for their excellent technical assistance. We also thank Prof. Robert Linsenmeier of Northwestern University and Dr. Howard Kruth of the National Institutes of Health for helpful discussions. This study is supported by NIH EY014662, NIH EY06109, American Health Assistance Foundation, International Retina Research Foundation, and the support to Department of Ophthalmology at UAB from Research to Prevent Blindness, Inc.

FIGURE LEGENDS

1. The LLPs seen in QFDE images of the EL of a 34 year-old eye. **(A)** The LLPs (arrows) have similar gray scale values as other ultrastructural features. **(B)** Particle content is cleared to make LLPs stand out. **(C)** After inverting and thresholding the image, only the LLPs remain. Scale bar = 100 nm.

2. The LLP volume fractions as a function of age in (**A**) ICL, (**B**) EL, and (**C**) OCL of BrM (n = 12 for **A** and **B**, n = 11 for **C**). **(D)** Comparison of OCL LLP volume fractions among different age groups. Asterisks indicate significant differences.

3. Comparison of the LLP volume fractions in the ICL, EL, and OCL of **(A)** 20-40 yr, (**B**) 40-60 yr, and (**C**) 60-80 yr eyes. Error bars show the standard deviations. Asterisks indicate significant differences.

4. The total quantity of LLP-associated lipids in BrM as a function of age.

5. The average LLP diameter as a function of age in **(A)** ICL, **(B)** EL, and **(C)** OCL.

6. The LLP diameter distribution in the different layers of BrM for younger eyes (20-40 yr old, solid blue line), middle aged eyes (40-60 yr old, dashed magenta line) and older eyes (60-80 yr old, dotted green line). n = 4 for all groups except for the data of OCL, 40-60 yr old (n = 3).

7. LLP particle diameter as a function of volume fraction in the different layers (all eyes).

References

1. Pauleikhoff D, Harper CA, Marshall J, Bird AC. Aging changes in Bruch's membrane. A histochemical and morphologic study. *Ophthalmology.* 1990;97:171-178.
2. Holz FG, Sheraidah G, Pauleikhoff D, Bird AC. Analysis of lipid deposits extracted from human macular and peripheral Bruch's membrane. *Arch. Ophthalmol.* 1994;112:402-406.
3. Curcio CA, Millican CL, Bailey T, Kruth HS. Accumulation of cholesterol with age in human Bruch's membrane. *Invest. Ophthalmol. Vis. Sci.* 2001;42:265-274.
4. Ruberti JW, Curcio CA, Millican CL, Menco BP, Huang JD, Johnson M. Quick-freeze/deep-etch visualization of age-related lipid accumulation in Bruch's membrane. *Invest. Ophthalmol. Vis. Sci.* 2003;44:1753-1759.
5. Huang JD, Presley JB, Chimento MF, Curcio CA, Johnson M. Age-related changes in human Bruch's membrane as seen by quick-freeze/deep-etch. In press at *Experimental Eye Research.*
6. Johnson M, Dabholkar A, Huang JD, Presley JB, Chimento MF, Curcio CA. Comparison of morphology of human macular and peripheral Bruch's membrane in old eyes. In press at *Current Eye Research.*
7. Marshall J, Hussain AA, Starita C, Moore DJ, Patmore AL. Ageing and Bruch's membrane. In Marmor MF, Wolfensberget TJ, eds. *Retinal Pigment Epithelium: Function and Disease.* New York, NY: Oxford University Press; 1998:669-692.
8. Sarks, SH. Ageing and degeneration in the macular region: a clinico-pathological study. *Br. J. Ophthalmol.* 1976;60:324-341.
9. Grindle CF, Marshall J. Ageing changes in Bruch's membrane and their functional implications. *Trans. Ophthalmol. Soc. U. K.* 1978;98:172-175.
10. Bird AC, Marshall, J. Retinal pigment epithelial detachments in the elderly. *Trans. Ophthalmol. Soc. U. K.* 1986;105:674-682.
11. Chen JC, Fitzke FW, Pauleikhoff D, Bird AC. Functional loss in age-related Bruch's membrane change with choroidal perfusion defect. *Invest. Ophthalmol. Vis. Sci.* 1992;33:334-340.
12. Starita C, Hussain AA, Pagliarini S, Marshall J. Hydrodynamics of aging Bruch's membrane: implications for macular disease. *Exp. Eye Res.* 1996;62:565-572.
13. Li CM, Chung BH, Presley JB, Malek G, Zhang X, Dashti N, Li L, Chen J, Bradley K, Kruth HS, Curcio CA, Lipoprotein-like particles and cholesteryl esters in human Bruch's membrane: initial characterization. *Invest. Ophthalmol. Vis. Sci.* 2005;46:2576-2586.
14. Curcio CA, Presley JB, Millican CL, Medeiros NE. Basal deposits and drusen in eyes with age-related maculopathy: evidence for solid lipid particles. *Exp. Eye. Res.* 2005;80:761-775.
15. Overby DR, Johnson M. Studies on depth-of-field effects in microscopy supported by numerical simulations. *J Microsc.* 2005;220:176-189.
16. Overby D, Ruberti J, Gong H, Freddo TF, Johnson M. Specific hydraulic conductivity of corneal stroma as seen by quick-freeze/deep-etch. *J. Biomech. Eng.* 2001;123:154-161.
17. Tso P, Ragland JB, Sabesin SM. Isolation and characterization of lipoprotein of density less than 1.006 g/ml from rat hepatic lymph. *J Lipid Res.* 1983;24:810-820.
18. Schmitz G, Assmann G, Augustin J, Dirkes-Kersting A, Brennhausen B, Karoff C. Characterization of very low density lipoproteins and intermediate density lipoproteins of normo- and hyperlipidemic apolipoprotein E-2 homozygotes. *J Lipid Res.* 1985;26:316-326.
19. Chapman MJ, Laplaud PM, Luc G, Forgez P, Bruckert E, Goulinet S, Lagrange D. Further resolution of the low density lipoprotein spectrum in normal human plasma:

physicochemical characteristics of discrete subspecies separated by density gradient ultracentrifugation. *J Lipid Res*. 1988;29:442-458.

20. Rifai N, Bachorik PS, Albers JJ. Lipids, lipoproteins, and apolipoproteins. In Burtis CA, Ashwood ER, eds. *Tietz Textbook of Clinical Chemistry*. Philadelphia, PA: W.B. Saunders Company; 1999:809-861.
21. Smith EB, Slater RS. Relationship between plasma lipids and arterial tissue lipids. *Nutr Metab.* 1973;15:17-26.
22. Haimovici R, Gantz DL, Rumelt S, Freddo TF, Small DM. The lipid composition of drusen, Bruch's membrane, and sclera by hot stage polarizing light microscopy. *Invest Ophthalmol Vis Sci*. 2001; 42:1592-1599.
23. Ethier CR, Johnson M, Ruberti J. Ocular biomechanics and biotransport. *Annu Rev Biomed Eng*. 2004; 6:249-273.

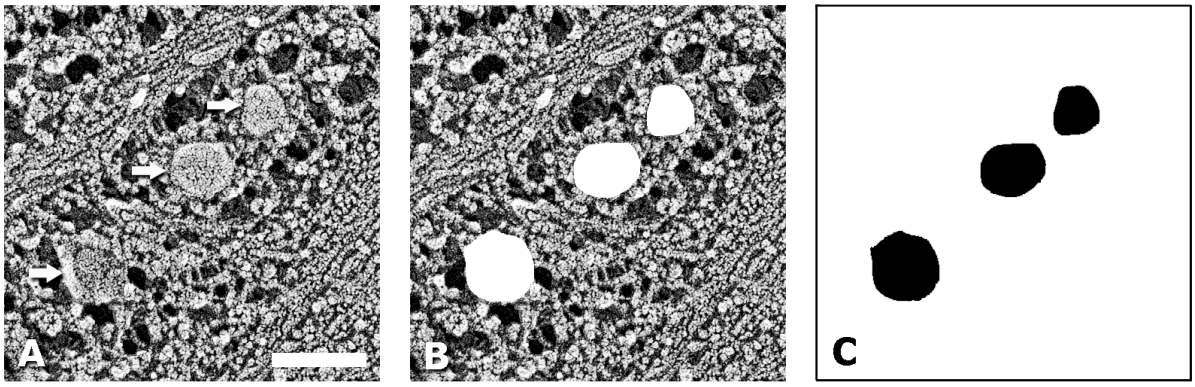


Figure 1

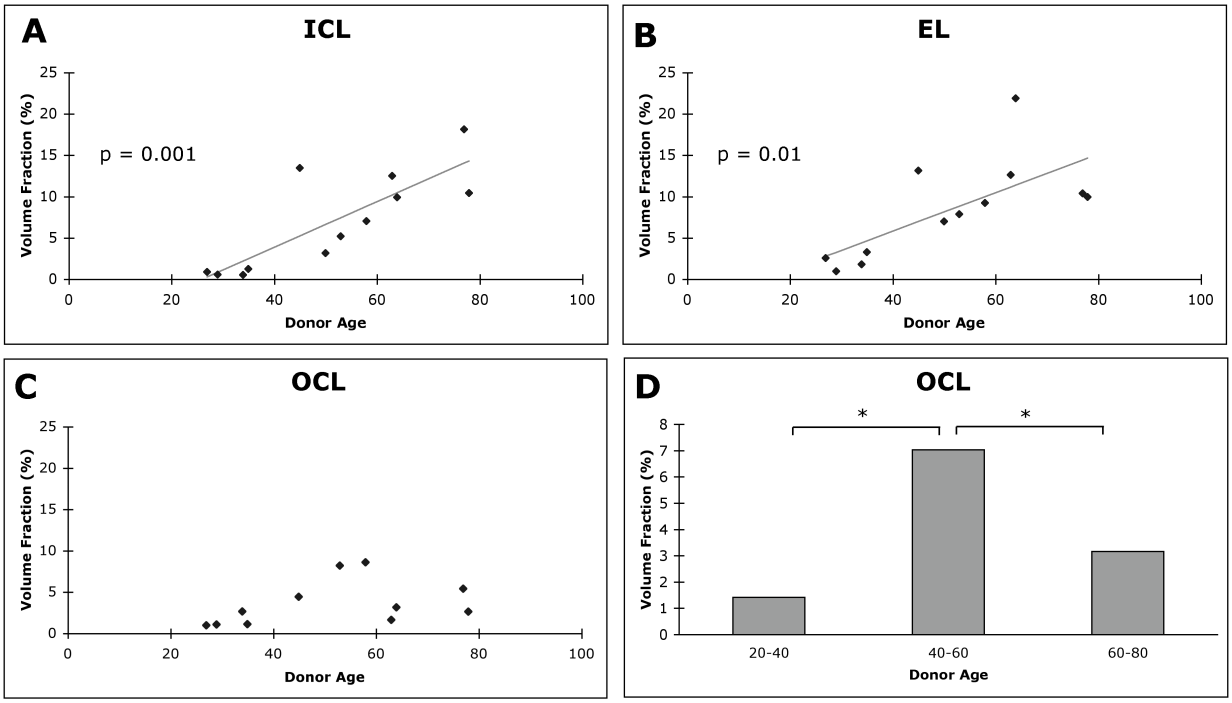

A
ICL
p = 0.001
Volume Fraction (%)
Donor Age
B
EL
p = 0.01
Volume Fraction (%)
Donor Age
C
OCL
Volume Fraction (%)
Donor Age
D
OCL
*
*
Volume Fraction (%)
20-40
40-60
60-80
Donor Age

Figure 2

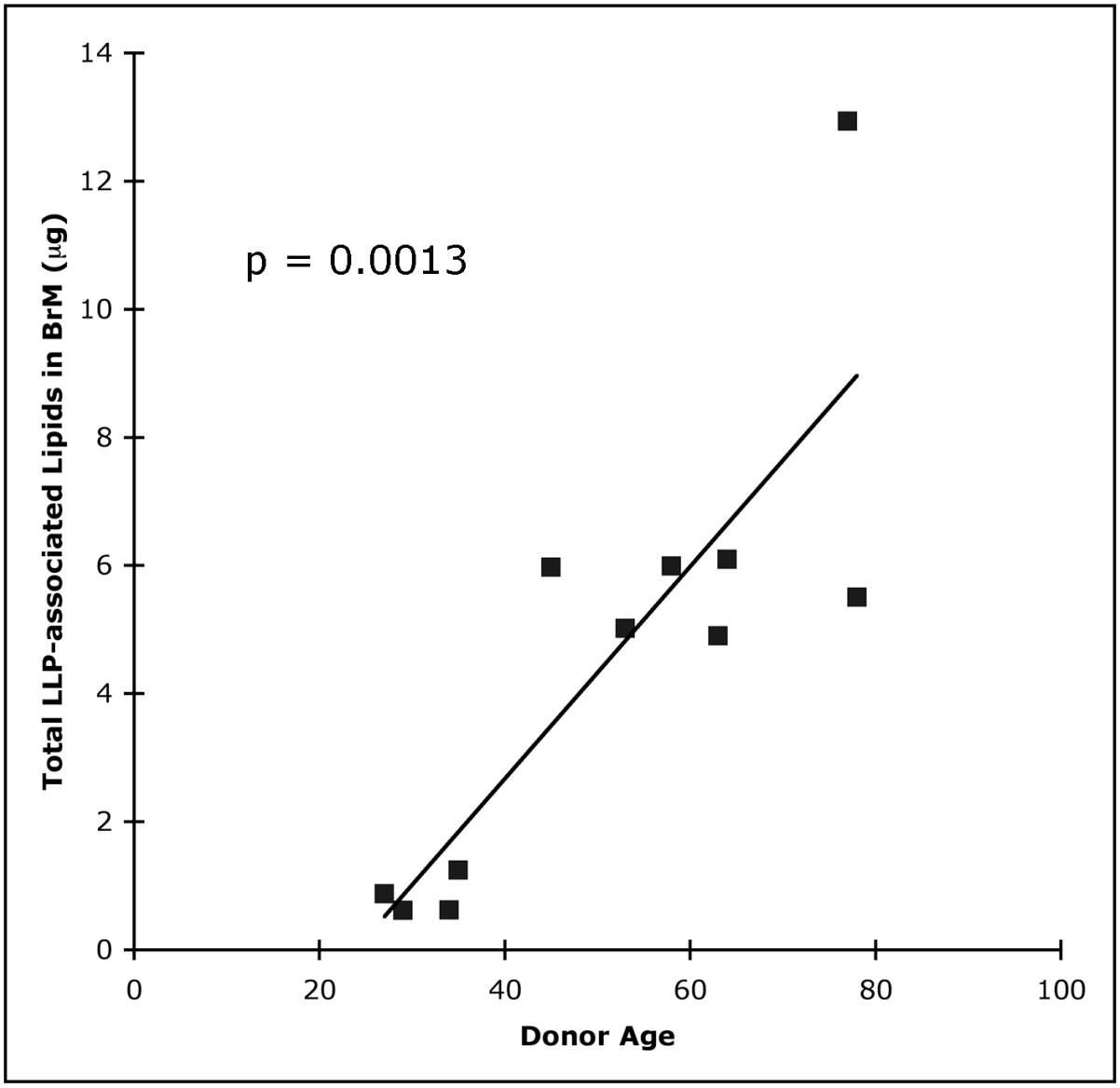

p = 0.0013
Total LLP-associated Lipids in BrM (μg)
Donor Age
0
2
4
6
8
10
12
14
0
20
40
60
80
100

Figure 4

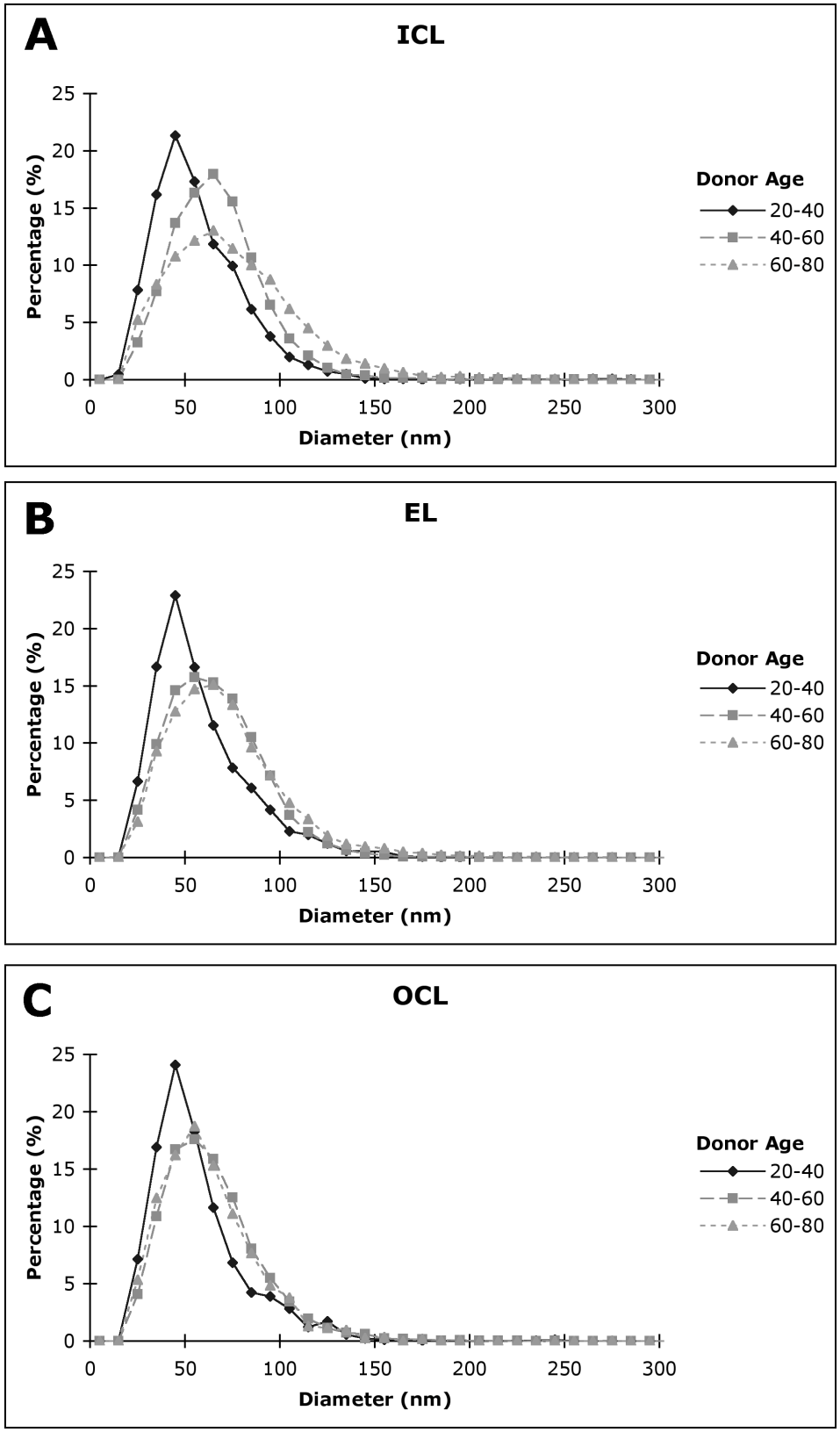

A
ICL
Percentage (%)
Diameter (nm)
Donor Age
20-40
40-60
60-80
B
EL
Percentage (%)
Diameter (nm)
Donor Age
20-40
40-60
60-80
C
OCL
Percentage (%)
Diameter (nm)
Donor Age
20-40
40-60
60-80

Figure 6

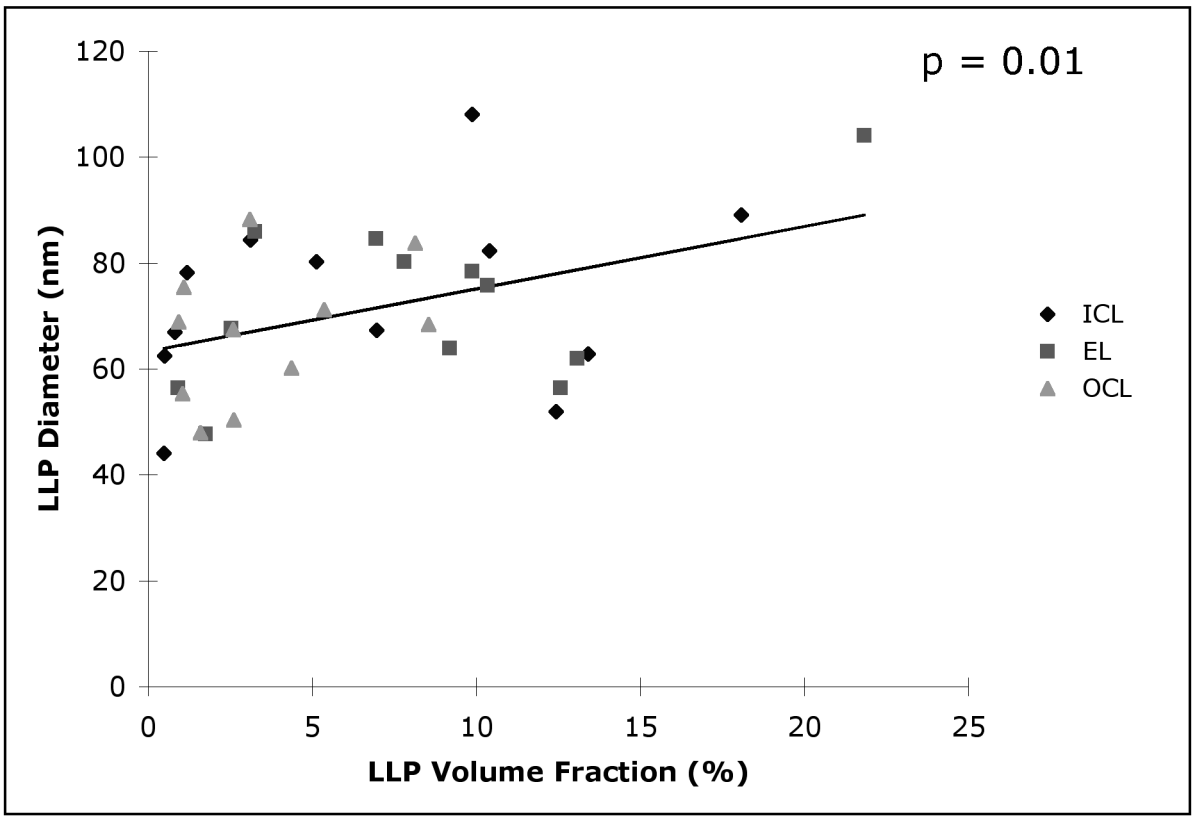

p = 0.01
LLP Diameter (nm)
LLP Volume Fraction (%)
0
20
40
60
80
100
120
0
5
10
15
20
25
ICL
EL
OCL

Figure 7

TABLE 1: Sample Eyes

Donor age	Gender	Ethnicity
27	F	AA
29	M	C
34	F	C
35	F	C
45	M	C
50	M	C
53	M	C
58	F	C
63	M	C
64	M	AA
77	F	C
78	M	C

NOTES

F = Female, M = Male

C = Caucasian, AA = African American

TABLE 2: Depth of field (D_f) and LLP volume fraction (ϕ) measured by image analysis

	ICL		EL		OCL	
Sample Age	D_f (nm)	ϕ	D_f (nm)	ϕ	D_f (nm)	ϕ
27	88.5	0.008	75.1	0.025	98.5	0.009
29	49.5	0.005	79.5	0.009	57.5	0.010
34	78.7	0.005	55.1	0.018	43.4	0.026
35	50.1	0.012	71.0	0.033	58.1	0.011
45	46.5	0.134	73.9	0.131	47.1	0.044
50	71.8	0.031	57.3	0.070	N/A	N/A
53	59.2	0.051	67.6	0.078	59.9	0.082
58	97.9	0.070	89.2	0.092	88.2	0.086
63	69.5	0.124	58.6	0.126	98.7	0.016
64	59.5	0.099	39.5	0.218	49.3	0.031
77	48.8	0.181	48.7	0.103	57.8	0.054
78	53.9	0.104	43.5	0.099	55.2	0.026

Note
N/A: not available